

Application of the Multiple Scattering $X\alpha$ Molecular Orbital Method to the Determination of the Electronic Structure of Metallocene Compounds. 1. Dibenzenechromium and Its Cation

Jacques Weber,*^{1a} Michel Geoffroy,^{1a} Annick Goursot,^{1b} and Edouard Pénigault^{1b}

Contribution from the Département de Chimie Physique, Université de Genève, 1211 Genève 4, Switzerland, and the Laboratoire de Photochimie Générale (E.R.A. No 336), Ecole Supérieure de Chimie de Mulhouse, 68093 Mulhouse Cedex, France. Received July 5, 1977

Abstract: Molecular orbital calculations using the all-electron self-consistent-field multiple scattering $X\alpha$ method have been carried out for $\text{Cr}(\text{C}_6\text{H}_6)_2$ and its cation. In both ground-state electronic structures, the level ordering for the highest occupied orbitals and the lowest unoccupied one is found to be $e_{1u}(\pi\text{-C}_6\text{H}_6) < e_{1g}(\pi\text{-C}_6\text{H}_6) < e_{2g}(3d) < a_{1g}(3d) < e^*_{1g}(3d)$ in agreement with several experimental measurements. The calculated ionization energies of $\text{Cr}(\text{C}_6\text{H}_6)_2$ agree very well with photoelectron data and for both compounds the calculated electronic excitation energies lead to a very satisfactory interpretation of optical and UV absorption spectra.

Introduction

In recent years, the chemistry of organometallic compounds of metallocene type has proved to be a subject of considerable interest. Particular emphasis has been placed on the understanding of their structure on the basis of both experimental² and theoretical³ work. Among the experimental techniques mostly used to this end, let us mention optical, UV, and photoelectron spectroscopy, electron spin resonance, magnetic susceptibility measurements, and x-ray structure determinations. Owing to the refinements recently brought to these techniques, a considerable amount of accurate data for metallocenes is now available. However, a coherent interpretation of these results is still lacking in many cases and there is no doubt that reliable molecular orbital (MO) calculations in this field would be most welcome. As examples they could bring answers to the controverted questions of the relative ordering of the d orbitals and of the assignment of the low-energy part of the electronic absorption spectra, provided that the method has been previously tested for some typical metallocene, like ferrocene ($\text{Fe}(\text{C}_5\text{H}_5)_2$), for which there are ample experimental data.

Several calculations have been performed for ferrocene by various MO methods,⁴⁻¹⁴ and the results can be summarized as follows. Semiempirical Hartree-Fock (HF) methods⁴⁻¹⁰ show the same drawback as in many other calculations on transition metal compounds: the relative ordering of the highest occupied valence orbitals is greatly dependent on the approximations inherent in the model; moreover, these methods are unsuitable for the assignment of the electronic absorption spectrum owing to the poor results they give for the energies of unoccupied levels. As to ab initio self-consistent field (SCF) calculations, Bagus et al.¹¹ have shown that a basis set of at least double ζ quality is necessary for obtaining ionization energies showing quantitative agreement with experiment, the minimum basis set used by Coutière et al.¹² leading to an overestimation of the binding energies by 2-3 eV. However, it is fair to mention that both calculations predict the same assignments for the lowest ionization energies of ferrocene and they are in this respect in agreement with the photoelectron data of Rabalais et al.¹⁵ An important problem occurring in all the Hartree-Fock calculations on ferrocene (and on metallocenes in general) is that Koopmans' theorem is not valid for such compounds:^{11,12} the sequence of ionization energies, calculated by the $\Delta E(\text{SCF})$ procedure (i.e., subtracting total

energies obtained in separate SCF calculations on the ion and the neutral molecule), is different from the sequence of orbital energies. This means that the calculation of each ionization energy requires a separate SCF calculation for the corresponding configuration of the cation and thus the ab initio procedure results in considerable amount of computer time when applied to metallocenes. Finally, two calculations on ferrocene using different versions of the Hartree-Fock-Slater $X\alpha$ (HFS $X\alpha$) method¹⁶ appeared recently.^{13,14} Their results are generally in good agreement with experiment: whereas the discrete variational (DV) $X\alpha$ model¹³ leads to ionization energies showing roughly the same agreement with experiment as those obtained from ab initio calculations with the extended basis set,¹¹ the multiple scattering (MS) $X\alpha$ scheme¹⁴ gives a very satisfactory interpretation of the optical absorption spectrum. In addition to its ability of describing adequately the electronic structure of large clusters like ferrocene, the HFS $X\alpha$ model has the advantage of requiring a much smaller amount of computer time than the ab initio technique. Furthermore, a simpler procedure than the $\Delta E(\text{SCF})$ one may be used for the determination of the ionization energies taking into account electronic relaxation effects. It is therefore interesting to apply this model to other metallocenes in order to test further its ability of predicting the electronic structure and related properties of these organometallics. In this work, the MS $X\alpha$ model¹⁷ is used for the calculation of the electronic structure of the most prominent of bisarene metal complexes, namely, dibenzenechromium, $\text{Cr}(\text{C}_6\text{H}_6)_2$, and its cation. The choice of dibenzenechromium is justified by the large number of experimental investigations which have been recently reported¹⁸⁻²⁹ for this compound, for some of which a theoretical confirmation of the interpretation of the data is still needed. Whereas it is now firmly established on the basis of low-temperature crystal data,¹⁸ electron diffraction measurements,¹⁹ and vapor phase infrared study²⁰ that $\text{Cr}(\text{C}_6\text{H}_6)_2$ has an eclipsed structure of sandwich type (D_{6h} symmetry) with planar C_6H_6 ligands, reliable MO calculations supporting the interpretation of photoelectron²¹⁻²⁴ and electronic absorption^{3,25} spectra have yet to be presented. Similarly, an MS $X\alpha$ study of the cation $\text{Cr}(\text{C}_6\text{H}_6)_2^+$ would be of interest in helping interpret both the ESR measurements²⁶ and the electronic absorption spectrum^{25,27-29} for which a tentative assignment of the main features has been reported by Warren.³

Several MO calculations have already been performed for $\text{Cr}(\text{C}_6\text{H}_6)_2$,^{9,24,30-33} but their results are not very useful when

trying to solve the problems mentioned above. Semiempirical calculations^{9,30-33} lead to results which are at considerable variance concerning ordering and energy separations of the highest occupied and lowest unoccupied molecular orbitals. On the other hand, the ab initio calculation of Guest et al.²⁴ predicts an incorrect sequence for the two lowest ionization energies, even in the $\Delta E(\text{SCF})$ procedure, when compared with the experimental assignment.^{21,24} This is undoubtedly due to the minimum basis set used by these authors in their calculation. Furthermore, this publication does not report the one-electron energies obtained for the virtual MO levels, so that it cannot be used, even from a qualitative point of view, for an interpretation of optical and UV absorption spectra. In consideration of all the deficiencies of these previous calculations, we found it worthwhile to perform new MO calculations for $\text{Cr}(\text{C}_6\text{H}_6)_2$ and $\text{Cr}(\text{C}_6\text{H}_6)_2^+$, using the MS $X\alpha$ model. As this method has recently been shown to be able to describe accurately the electronic structure of transition metal complexes³⁴⁻³⁶ and heavy metal compounds,³⁷⁻³⁹ we can be reasonably confident in its ability of predicting the electronic properties of dibenzenechromium. A description of the computational details as well as a justification of our choice of MS $X\alpha$ parameters are presented in the next section.

Computational Details and MS $X\alpha$ Parameters

The standard version of the SCF MS $X\alpha$ method¹⁷ is used. This model has been described in detail several times^{16,17,40} and it does not need further development here. However, some computational details as well as the choice of the calculation parameters deserve some comments since they have been shown to possibly have a nonnegligible influence on the results.^{36,41,42}

In all the calculations performed for dibenzenechromium and its cation, the experimental geometry¹⁹ of $\text{Cr}(\text{C}_6\text{H}_6)_2$ is used, i.e., an eclipsed structure of D_{6h} symmetry with planar C_6H_6 ligands, the bond lengths being C-C 1.423 Å, C-H 1.090 Å, and the vertical ring to ring distance 3.226 Å.

It is well known that two kinds of parameters appear in the MS $X\alpha$ model: (1) the exchange parameter α , which is allowed to have different values in the various regions of the muffin-tin partitioning of the molecule, and (2) the radii of muffin-tin spheres centered on the nuclei. Whereas choosing the α parameters is a straightforward problem since their atomic values have been optimized by Schwarz,^{43,44} the choice of appropriate values for the radii of atomic spheres may be delicate, since it is enlarged by the possibility of using overlapping, instead of "touching", atomic spheres⁴⁵ in an attempt of circumventing the limitations of the muffin-tin approximation. The influence of this choice on the results has been recently investigated for various compounds by one of us,^{36,41,42} leading to the conclusion that, when modifying the spheres radii, nonuniform shifts of the electronic levels of several electron volts and, in some cases, valence level crossings may occur. Thus it seems preferable to perform several calculations using different sets of spheres radii, the criterion for selecting the best set being undoubtedly a comparison between the results obtained in each case and experiment. Owing to the nature of the $\text{Cr}(\text{C}_6\text{H}_6)_2$ molecule, it is reasonable to use in a first step a trial set of parameters in which the spheres radii of one ligand C_6H_6 are chosen as those optimized in preliminary calculations performed for C_6H_6 itself, in agreement with the procedure used by Rösch and Johnson¹⁴ for ferrocene. As shown by Rösch et al.,⁴⁵ it was found that an excellent agreement with experiment is obtained for the ionization energies of benzene when using overlapping atomic spheres and an additional "empty" sphere located in the middle of the ring (a detailed account of these results will be presented in the next section). Then, after a scaling of their values due to the slightly modified geometry of the benzene rings in $\text{Cr}(\text{C}_6\text{H}_6)_2$, we have used in the first test

Table I. MS $X\alpha$ Parameters for Benzene

$X\alpha$ exchange parameter	Sphere radii, au				
	A	B	C		
α_{C}	0.753 31	R_{C}	1.318 10	1.647 63	1.647 63
α_{H}	0.777 25	R_{H}	0.732 28	0.915 35	0.915 35
$\alpha_{\text{sphere}}^{\text{outer}}$	0.765 28	$R_{\text{sphere}}^{\text{outer}}$	5.418 86	5.601 93	5.601 93
$\alpha_{\text{sphere}}^{\text{empty}}$	0.765 28	$R_{\text{sphere}}^{\text{empty}}$			1.318 10
$\alpha_{\text{sphere}}^{\text{inter}}$	0.765 28				

Table II. MS $X\alpha$ Parameters for $\text{Cr}(\text{C}_6\text{H}_6)_2$

Region	$X\alpha$ exchange parameter	Sphere radii, au
Cr atom	0.713 52	1.703 61
C atom	0.753 31	1.680 70
H atom	0.777 25	0.894 09
Empty sphere	0.763 21	1.344 56
Outer sphere	0.763 21	6.537 13
Intersphere	0.763 21	

calculation for dibenzenechromium the same sphere radii as those determined for benzene, the radius of the chromium sphere being chosen such as to be "touching" with the "empty" spheres of both C_6H_6 ligands. When comparing with experiment the electronic structure of $\text{Cr}(\text{C}_6\text{H}_6)_2$ obtained with this parameter set, we have found that ligand orbitals have both proper ordering and correct spacings. Furthermore, as presented in the next section, their calculated ionization energies are in very good agreement with experiment. Therefore we have found it useless to modify the radii of carbon and hydrogen spheres and in a second calculation the radius of chromium sphere was increased by 25%. The results obtained in this second case are not reported here: they are very similar to those obtained in the first calculation, indicating upwards shifts of the levels by a few tenths of an electron volt and differences in the electronic distributions of a few percent. As the results obtained with the smaller radius of chromium sphere lead to a slightly more reasonable distribution of the total electronic charge in the complex, it is preferable to present them in this work in view of the importance of a correct charge distribution in an attempt at explaining the chemical bonding in $\text{Cr}(\text{C}_6\text{H}_6)_2$.

Table I presents the values of the MS $X\alpha$ parameters used in the preliminary calculations performed for benzene (the geometry of C_6H_6 was taken from ref 46: bond lengths C-C 1.395 Å and C-H 1.085 Å). The atomic exchange parameters α are those used by Rösch et al.⁴⁵ in the spin-unrestricted case, whereas the arithmetic mean of these values is chosen for the α value outside the atomic spheres. Three different sets of sphere radii are considered. Parameter set A corresponds to nonoverlapping ("touching") atomic spheres, whose radii are fixed by the geometry. Parameter set B is generated from set A by increasing the radii of atomic spheres by 25%. Leading to moderate amount of spheres overlapping, this procedure has been shown to give generally the optimum choice of radii for neutral compounds.^{36,42} Finally, set C is merely set B enlarged by an empty sphere (i.e., a region of spherically averaged, instead of constant, potential and charge density which does not contain a nuclear charge) located in the center of the molecule with a radius equal to that of the carbon sphere of set A. An externally tangent outer sphere is used in each calculation.

The MS $X\alpha$ parameters used for $\text{Cr}(\text{C}_6\text{H}_6)_2$ are displayed in Table II. It is to be noticed that we used for the cation $\text{Cr}(\text{C}_6\text{H}_6)_2^+$ the same set of parameters as for the neutral species itself. The atomic exchange parameters α for carbon and hydrogen are those used in the C_6H_6 calculation, whereas

Table III. Ground-State Energy Levels^a (Ry) for Benzene Calculated with Parameters Sets A, B, and C

Level	Energy		
	A	B	C
2a _{2u}	-0.269	-0.065	-0.053
4a _{1g}	-0.370	-0.129	-0.114
1e _{2u}	-0.421	-0.092	-0.054
1e _{1g}	-0.762	-0.493	-0.452
3e _{2g}	-0.844	-0.682	-0.647
1a _{2u}	-0.948	-0.706	-0.665
3e _{1u}	-0.952	-0.823	-0.810
2b _{1u}	-1.005	-0.850	-0.820
1b _{2u}	-1.084	-0.989	-0.938
3a _{1g}	-1.119	-1.003	-1.001
2e _{2g}	-1.320	-1.213	-1.168
2e _{1u}	-1.571	-1.479	-1.448
2a _{1g}	-1.751	-1.690	-1.693
1b _{1u}	-20.387	-19.872	-19.844
1e _{2g}	-20.387	-19.872	-19.844
1e _{1u}	-20.387	-19.872	-19.844
1a _{1g}	-20.387	-19.872	-19.844

^a The highest occupied level is 1e_{1g}.

the α value for chromium is taken from the tabulation of Schwarz.⁴³ A weighted average of the atomic values (12 parts of carbon and hydrogen to 1 part of chromium) is chosen for the α value in interatomic, extramolecular, and empty spheres regions. The atomic sphere radii of carbon and hydrogen as well as the radii of empty spheres are those of set C of the benzene calculation, scaled according to the changes in the C-C and C-H bond lengths. The chromium sphere is taken "touching" with the empty spheres and, as usual, the extramolecular region is delimited by an externally tangent outer sphere.

In all the calculations, partial waves up to $l = 2$ are included in the multiple scattering expansions in the chromium sphere and extramolecular region, up to $l = 1$ in carbon and empty spheres, and up to $l = 0$ in hydrogen sphere.⁴⁷ The effect of an external stabilizing electrostatic field on the cation $\text{Cr}(\text{C}_6\text{H}_6)_2^+$ is taken into account by use of a Watson sphere of the same radius as the outer sphere and bearing a charge of -1 . The MS X α method being an all-electron MO model, the inner shell electrons are also allowed to adjust their one-electron energies during the SCF procedure, but they are constrained to conserve their atomic character and to be entirely localized within the atomic spheres ("thawed" core approximation). The transition state method⁴⁸ is used for the determination of ionization energies and excitation energies. All the calculations are performed using the non-spin-polarized version of the MS X α computer programs. When considering an electronic excitation, we calculate thus an average over multiplet states arising from the given electronic configuration, since in the HFS X α model the determination of the energy splitting between multiplet states of the same multiplicity requires additional spin-polarized calculations.³⁶

Results and Discussion

Benzene. Summarized in Table III are the ground-state energy levels for benzene calculated with parameter sets A, B, and C. In each case, the highest occupied level is 1e_{1g} (π). Whereas the ordering of all the occupied levels is the same in the three calculations, it is seen that there is an inversion of the unoccupied levels 1e_{2u} (π^*) and 4a_{1g} (Rydberg 3s) in results B and C when compared with A. This is undoubtedly due to the fact that the potential in extramolecular and intersphere regions, where the virtual orbitals are for the most part localized, is more sensitive to the choice of spheres radii than the potential in atomic spheres themselves. Though we did not

Table IV. Theoretical and Experimental Ionization Energies (eV) for Benzene

Orbital	MS X α^a			Ab initio ^b	Expt ^c
	A	B	C		
1e _{1g}	13.36	9.61	8.98	9.08	9.25
3e _{2g}	14.48	12.20	11.66	13.46	11.49
1a _{2u}	15.86	12.49	11.86	13.55	12.0-12.3
3e _{1u}	15.95	14.11	13.88	16.0	13.8
1b _{2u}	17.84	16.56	15.78	16.8	14.5-14.7
2b _{1u}	16.63	14.42	13.95	17.5	15.2-15.4
3a _{1g}	18.18	16.53	16.46	19.3	16.84
2e _{2g}	20.99	19.52	18.83	22.4	18.7-19.2
2e _{1u}	24.41	23.16	22.68	27.6	22.0-22.8
2a _{1g}	26.87	26.04	26.05	31.3	28.7

^a This work, transition state energies. ^b Reference 46, Koopmans' theorem. ^c Reference 50.

attempt to calculate electronic excitation energies for benzene, the results of Table III suggest that the Rydberg transition $\pi(1e_{1g}) \rightarrow 3s$ should occur in the same region of the absorption spectrum as the first $\pi \rightarrow \pi^*$ bands, which is confirmed by a recent analysis of the UV spectrum of benzene.⁴⁹ Furthermore, the energy separation between 1e_{1g} (π) and 1e_{2u} (π^*) orbitals is about 5 eV in each calculation, in quantitative agreement with the lowest $\pi \rightarrow \pi^*$ transition derived from experiment.⁴⁹ Examination of Table III shows that when atomic spheres are allowed to overlap (i.e., going from A to B) the electronic levels are strongly shifted upwards, since a large amount of charge is transferred from the interatomic region into atomic spheres, increasing thus the Coulombic repulsion between electrons. However, this shift is nonuniform and the energy separations between the levels are quite different in both cases. Inserting the empty sphere (i.e., going from B to C) leads to small changes in orbital energies: the levels are slightly shifted upwards, the largest shifts being observed as expected for the orbitals which contribute the most to the charge in the interatomic region. As far as energy separations between occupied levels are concerned, a comparison with the near Hartree-Fock limit ab initio results of Ermler and Kern⁴⁶ shows that the MS X α results obtained using sets B and C are more realistic. This is further emphasized in Table IV, which presents a comparison between theoretical (MS X α , cases A, B, C; ab initio⁴⁶) and experimental⁵⁰ ionization energies of benzene.

From Table IV, it is clear that the use of overlapping, instead of "touching", atomic spheres leads to a considerable improvement of the MS X α ionization energies: whereas the binding energies obtained with parameters A are overestimated (except 2a_{1g}) by 2-4 eV, the energies resulting from set B are in much better agreement with experiment. When inserting the additional empty sphere (set C), the results are further improved and they are even superior to those obtained from the near Hartree-Fock limit ab initio calculation⁴⁶ using Koopmans' theorem. The only disagreement between MS X α results and experiment is related to the respective positions of the 1b_{2u} and 2b_{1u} molecular orbitals: whereas the interpretation of UV absorption and photoelectron spectra of benzene⁵⁰ as well as the ab initio results⁴⁶ suggest that the 1b_{2u} orbital lies above the 2b_{1u}, we obtain in all cases the opposite ordering. As Rösch et al.⁴⁵ in their MS X α calculations using parameters different from ours have obtained the same inversion, we conclude that this is an effect of the basic muffin-tin approximation. Nevertheless the MS X α electronic structure calculated with parameter set C is on the whole in good agreement with experiment, which clearly means that the same situation may be expected for the ligand molecular orbitals of $\text{Cr}(\text{C}_6\text{H}_6)_2$.

The Ground-State Electronic Structure of $\text{Cr}(\text{C}_6\text{H}_6)_2$. The electronic energy levels of the ground-state configuration

Table V. Ground-State Energy Levels^a (Ry) and Charge Distribution for Cr(C₆H₆)₂^b

Orbital	Energy	Charge distribution, ^c %									
		Cr			C			H	Empty sphere	Inter-sphere	Outer sphere
		s	p	d	s	pσ	pπ				
9a _{1g}	-0.089				4	1	4		1	39	51
5e _{2g}	-0.101			39			32			24	5
4e _{2u}	-0.110						74			26	
5e _{1g}	-0.129			75	1	2	10			10	2
8a _{1g}	-0.275			77		1		1	3	18	
4e _{2g}	-0.351			43		1	22			34	
4e _{1g}	-0.545			11			54			34	1
6e _{1u}	-0.579		1				49			50	
6a _{2u}	-0.675		1				62		1	33	3
3e _{2g}	-0.680				1	60		17		20	2
3e _{2u}	-0.682					60		17		23	
7a _{1g}	-0.749	1					57		1	38	3
3e _{1g}	-0.836			2		57		17	3	18	3
5e _{1u}	-0.840					58		17	3	19	3
2b _{2g}	-0.858				28	20		23		29	
2b _{1u}	-0.873				28	18		22		32	
1b _{1g}	-0.969					95				5	
1b _{2u}	-0.974					94				6	
5a _{2u}	-1.018				5	48		16	6	23	
6a _{1g}	-1.041			1	5	45		15	6	24	3
2e _{2u}	-1.203				46	34			6	14	
2e _{2g}	-1.213				46	34			6	14	
2e _{1g}	-1.492			1	74	11		3	2	8	1
4e _{1u}	-1.493				73	11		3	2	10	1
4a _{2u}	-1.714		1		76	9		1	9	4	
5a _{1g}	-1.737			1	75	9		1	9	5	
3e _{1u}	-3.462		96							4	
3a _{2u}	-3.469		95						1	4	
Cr 3s	-5.502	100									
C 1s	-19.923				100						
Cr 2p	-41.197		100								
Cr 2s	-48.362	100									
Cr 1s	-428.543	100									

^a The highest occupied level is 8a_{1g}. ^b The C, H and empty sphere charge distributions refer to the charge contained in *all* the respective spheres of the same type. ^c The analysis of charge distribution inside atomic spheres is made according to angular momentum contributions to the total charge inside these spheres.

¹A_{1g}(4e_{2g})⁴(8a_{1g})² of Cr(C₆H₆)₂ together with an analysis of their charge distribution in the various regions of the cluster are represented in Table V. It is seen that the sequence of predominantly metal 3d orbitals is 4e_{2g}(3dδ) < 8a_{1g}(3dσ) < 5e_{1g}(3dπ)⁵¹ with 8a_{1g} as the highest occupied MO and 5e_{1g} as the lowest unoccupied one. This ordering is in agreement with the general ligand field theory of such metal sandwich complexes.³ The 4e_{2g}(3dδ) MO is strongly bonding through in-phase combinations of metal 3dδ and ligand π orbitals, which is emphasized by its charge distribution analysis showing large participation of ligand π electrons. The bonding character of the 4e_{2g} MO is further strengthened by the fair amount of back-bonding occurring via the unoccupied 5e_{2g} MO, and the largest contribution to metal–ligand bonding in Cr(C₆H₆)₂ is thus provided by the 4e_{2g} MO. As to the 8a_{1g}(3dσ) MO, it is essentially nonbonding since it is localized only in the chromium sphere and, to a lesser extent, in the interatomic region. The unoccupied 5e_{1g}(3dπ) MO is strongly antibonding through out-of-phase combinations of metal 3dπ and ligand π orbitals.

It is interesting to remark that, in addition to confirming the qualitative conclusions of elementary ligand field theory,³ the MS X_α sequence of “d-like” molecular orbitals leads to a very good agreement with photoelectron, optical, and UV spectra, as will be shown in the next sections. However, this ordering differs markedly from that obtained in previous calculations: *ab initio*²⁴ and CNDO/2³³ results predict 8a_{1g} < 4e_{2g} for the occupied orbitals (no mention is made of the unoccupied 5e_{1g} MO), whereas a GTO–CNDO/2³² prediction leads to a

highest occupied orbital of metal 4p type. Extended Hückel calculations give the correct ordering 4e_{2g} < 8a_{1g}^{9,30,31} (though they are at considerable variance concerning the energy separation between these orbitals), but fail³¹ to predict 5e_{1g} as the lowest unoccupied orbital. In view of these poor results, it is easy to realize that none of these previous calculations may be used, even from a qualitative point of view, in an attempt to assign the optical and UV electronic absorption bands of Cr(C₆H₆)₂ and its cation.

The other occupied valence levels of Cr(C₆H₆)₂ are mainly ligand-type MOs grouped in pairs of in-phase and out-of-phase combinations of symmetry orbitals of C₆H₆: the 4e_{1g} MO, which reveals a substantial metal 3d component and contributes therefore to bonding interactions in the complex, and the 6e_{1u} MO correlate with the 1e_{1g} MO of benzene, the 6a_{2u} and 7a_{1g} with the 1a_{2u}, the 3e_{2g} and 3e_{2u} with the 3e_{2g}, and so on. It is seen from Table V that the fractions of orbital charge localized in the empty sphere and extramolecular region (outer sphere) are generally small, whereas the intersphere contribution decreases as expected when deeper levels are considered. The only notable exception to this statement is related to the virtual 9a_{1g} MO which has a large extramolecular component. This can be undoubtedly interpreted as the characteristic of a Rydberg-type orbital, probably of carbon 3s nature as may be inferred from the results obtained for benzene. The other unoccupied ligand-type MOs are 5e_{2g} and 4e_{2u}, which correlate with the 1e_{2u} MO of benzene.

Examination of Table V shows that metal s and p contributions to orbital charge of the bonding MOs are practically

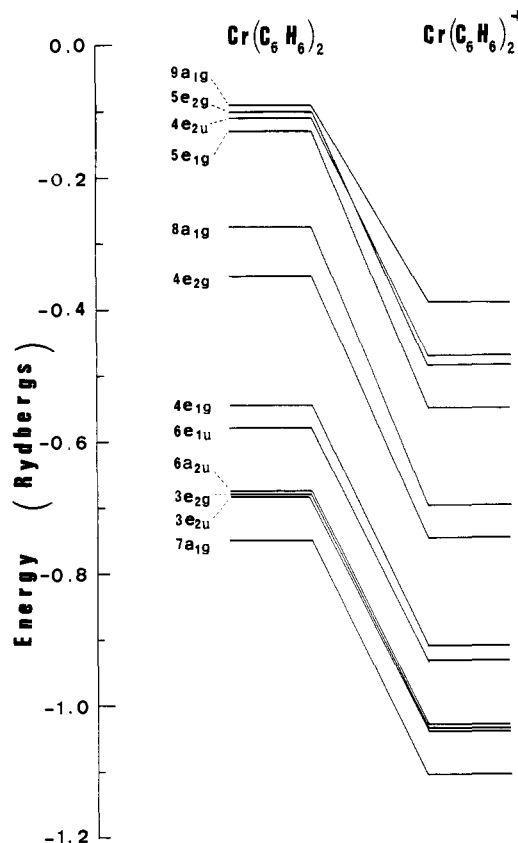
Table VI. Ground-State Total Electronic Charges (electronic charge units) in the Various Regions and Total Energies (Ry) for $\text{Cr}(\text{C}_6\text{H}_6)_2$ and $\text{Cr}(\text{C}_6\text{H}_6)_2^+$

	$\text{Cr}(\text{C}_6\text{H}_6)_2$	$\text{Cr}(\text{C}_6\text{H}_6)_2^+$
Electronic charge in		
Chromium sphere	21.670	21.630
Carbon sphere	5.422	5.420
Hydrogen sphere	0.420	0.414
Empty sphere	0.562	0.555
Interatomic region	14.432	13.669
Extramolecular region	0.672	0.584
Total energy	-3008.7250	-3008.2370

zero, which indicates that chromium 4s and 4p orbitals do not participate in the bonding and this is in agreement with the conclusions of Hillier et al.^{9,24} Similarly it is seen that the σ framework of ligands contributes very little to the bonding of the complex. The present calculations show again that $\text{Cr}(\text{C}_6\text{H}_6)_2$ is a transition metal π complex in which bonding interactions involve metal d and ligand $p\pi$ orbitals.

The highest occupied and lowest unoccupied MOs of $\text{Cr}(\text{C}_6\text{H}_6)_2$ and $\text{Cr}(\text{C}_6\text{H}_6)_2^+$ are represented in the orbital energy diagram of Figure 1. This will help in understanding the main differences in the electronic absorption spectra of both compounds, as will be discussed below. Table VI presents the distribution of total electronic charge among the various regions of the clusters $\text{Cr}(\text{C}_6\text{H}_6)_2$ and $\text{Cr}(\text{C}_6\text{H}_6)_2^+$. The results of Table VI are of course somewhat dependent on the radii of atomic spheres, as was the orbital charge distribution displayed in Table V. However, previous MS $X\alpha$ calculations⁴¹ performed for PO_4^{3-} have shown that the parameter set which gives the best agreement with experiment for ionization energies is also able to lead to a very reasonable charge distribution. We can thus reasonably expect that this conclusion is also valid for $\text{Cr}(\text{C}_6\text{H}_6)_2$ and a test of the quality of our charge distribution analysis will now be performed by estimating the atomic charge of chromium in the ground state of the neutral complex.

As the results of Table V indicate that no chromium 4s or 4p electrons take part in the ground-state configuration, the problem of estimating the charge of chromium reduces to that of finding the total metal 3d population from an analysis of the MOs $4e_{1g}$, $4e_{2g}$, and $8a_{1g}$. A difficulty then arises when considering the large components of interatomic charge exhibited by these orbitals: 34% ($4e_{1g}$, $4e_{2g}$) and 18% ($8a_{1g}$), since there is no unambiguous way of assigning this important charge to the various atoms of the complex. Indeed the chromium configuration is $3d^{3.70}$ ($d_{z^2}^{1.54}$, $d_{x^2-y^2}^{0.86}$, $d_{xz}^{0.22}$) when taking into account only the charge distribution analysis inside the metal sphere for the MOs $4e_{1g}$, $4e_{2g}$, $8a_{1g}$, and it is thus obvious that part of the intersphere charge must be assigned somehow to the chromium atom. Johnson¹⁷ has suggested distributing the interatomic charge *equally* among all atoms in the molecule, but this procedure is inapplicable to our problem because the interatomic charge should be shared between 25 atoms, each of them receiving a negligible amount of additional charge. We suggest thus the alternative of distributing for each orbital the interatomic charge among all atoms in the molecule *proportionally* to the amount of orbital charge (originating from this MO) included in each sphere. This leads to the more realistic configuration $3d^{5.14}$ ($d_{z^2}^{1.88}$, $d_{x^2-y^2}^{1.30}$, $d_{xz}^{0.33}$) for chromium, the charge on this atom being thus +0.86, resulting from (1) a transfer of 0.66e from $2p\pi$ orbitals of benzene rings to metal orbitals d_{xz} and d_{yz} and (2) a back-bonding transfer of 1.52e from metal d_{z^2} , $d_{x^2-y^2}$, d_{xy} to ligand $2p\pi$ orbitals. The MS $X\alpha$ formal charge of Cr (+0.86) in $\text{Cr}(\text{C}_6\text{H}_6)_2$ seems a reasonable result for such a neutral and nonionic compound.³ Furthermore, it is in qualitative agreement with an ESCA study of

**Figure 1.** Ground-state valence energy levels for $\text{Cr}(\text{C}_6\text{H}_6)_2$ and $\text{Cr}(\text{C}_6\text{H}_6)_2^+$. The highest occupied level is $8a_{1g}$, which accommodates two electrons in $\text{Cr}(\text{C}_6\text{H}_6)_2$ and one electron in the cation.

chemical shifts in several bis(arene)chromium complexes,²² showing that the Cr atom in $\text{Cr}(\text{C}_6\text{H}_6)_2$ carries a partial positive charge, and with the previous theoretical estimations of Hillier and Canadine⁹ (+0.54) and Fitzpatrick et al.³³ (from +0.49 to +0.41 depending on the geometry used). In fact, a charge of +0.86 on Cr is a more realistic estimation than the *ab initio* result of +2.66 found by Guest et al.²⁴ (such an excessive value could be attributed to an effect of the minimum basis set used by these authors) and the GTO-CNDO/2 result of -0.22 obtained by Saillard et al.³² (this negative value may be attributed to the questionable electronic structure predicted in this work).

Ionization Energies of $\text{Cr}(\text{C}_6\text{H}_6)_2$. The MS $X\alpha$ ionization energies I of $\text{Cr}(\text{C}_6\text{H}_6)_2$ as calculated taking into account the major part of relaxation effects by use of the transition state procedure⁴⁸ and corresponding UV and x-ray photoelectron data obtained by various authors²¹⁻²⁴ are presented in Table VII. It is seen that the agreement between calculated and observed values is very good for both valence and core orbitals. In agreement with the interpretation of UV photoelectron spectra proposed by Evans et al.²¹ and Guest et al.,²⁴ the two low-energy bands are calculated to result from ionization of metal d electrons, the sequence $I(8a_{1g}) < I(4e_{2g})$ being the same as that deduced from an analysis of band intensities. It is interesting to observe that the opposite ordering has been obtained by Guest et al.²⁴ in their *ab initio* calculation, even when using the $\Delta E(\text{SCF})$ procedure (i.e., when taking into account relaxation effects), which is attributed by these authors to an inadequate chromium 3d basis. Aside from a correct ordering of metal 3d ionization energies, the experimental energy difference between the corresponding bands (1 eV) is fairly well reproduced in the MS $X\alpha$ calculations (0.73 eV). All the features beyond 8 eV in the UV photoelectron spectra have been attributed^{21,24} to ionization of electrons predomi-

Table VII. Comparison between MS X α Ionization Energies (eV) Calculated for Cr(C₆H₆)₂ and Experimental Values

Orbital	MS X α	Expt			
		Ref 24 ^a	Ref 21	Ref 23	Ref 22 ^b
8a _{1g}	6.60	5.45	5.4	5.7	
4e _{2g}	7.33	6.46	6.4		
4e _{1g}	9.83	9.56 (sh)	9.6		
6e _{1u}	10.24	9.80			
6a _{2u}	11.57	11.39			
3e _{2g}	11.63	11.9 (sh)	11.5		
3e _{2u}	11.66				
7a _{1g}	12.57	12.7 (sh)			
3e _{1g}	13.75				
5e _{1u}	13.81	14.23	13.8		
2b _{2g}	14.04				
2b _{1u}	14.24				
1b _{1g}	15.63	15.2 (sh) ^c			
1b _{2u}	15.70				
5a _{2u}	16.23	16.83			
6a _{1g}	16.54				
2e _{2u}	18.80	18.68			
2e _{2g}	18.92				
2e _{1g}	22.84	23.2			
4e _{1u}	22.85				
3e _{1u} (Cr 3p)	50.3				
3a _{2u} (Cr 3p)	50.4		49.4 ^b	49.2	
Cr 3s	78.1		80.6 ^b	80.5	
Cr 2p	580.9				582.5 ^d

^a sh = shoulder. ^b X-ray photoelectron measurements performed on solid Cr(C₆H₆)₂. Corresponding ionization energies are given relative to *vacuum* using the value 290.4 eV⁵² for carbon 1s binding energy of gaseous C₆H₆. ^c There is a misprint in the corresponding value of ref 24 (14.2 eV). Examination of the spectrum shows that this value should be read 15.2 eV. ^d Center of gravity of the 2p_{1/2} and 3p_{3/2} binding energies of ref 22.

nantly localized on ligands, whose orbitals are grouped in pairs of in-phase and out-of-phase combinations of benzene orbitals. This interpretation is confirmed by our calculations and this is clearly reflected by the results displayed in Table VII. The third band of the spectrum, corresponding to ionizations from the ligand π 4e_{1g} and 6e_{1u} MOs, is predicted to have two components at 9.83 and 10.24 eV, in excellent agreement with the experimental values of 9.80 for band maximum and 9.56 for the shoulder. In the photoelectron spectrum,²⁴ the next band is broad with a maximum at 11.39 eV and a large splitting of 1.31 eV; the calculations show that this is due to photoemission from two pairs of ligand levels (6a_{2u}, 7a_{1g}; 3e_{2g}, 3e_{2u}) with a maximum in the region 11.6–12.6 eV and a splitting of 1.0 eV. When examining in Table VII the MS X α binding energies obtained for deeper valence levels (with corresponding maxima in the UV photoelectron spectrum²⁴ at 14.23, 15.2 (shoulder), 16.83, 18.68, and 23.2 eV), it is seen that the agreement with experiment is again excellent, the discrepancy being in each case a few tenths of an electron volt. There is no doubt that this qualitative agreement with experiment for binding energies of ligand electrons is mainly to be attributed to our procedure of optimizing in a first step the parameters for benzene.

As to chromium inner shell binding energies, it is seen from Table VII that the MS X α predictions are also in good agreement with x-ray photoelectron data. The theoretical result concerning the chromium 2p binding energy is particularly accurate since the discrepancy with experiment (582.5 eV) is only 1.6 eV. As a conclusion, let us mention that the ionization energies presented above indicate that the electronic structure of occupied levels of Cr(C₆H₆)₂ is fairly well described by the MS X α model. Indications concerning the degree of accuracy of the electronic structure of unoccupied levels are provided

Table VIII. Comparison between Electronic Excitation Energies (cm⁻¹) Calculated for Cr(C₆H₆)₂ and Experimental Values of Peak Positions

Transition ^a	Type of transition ^b	Calcd value	Exptl peak position ^c
8a _{1g} → 5e _{1g} (A)	d → d	16 050	15 600
8a _{1g} → 5e _{2g} (F)	d → d; CT - (M → L) ^d	20 000	(24 000)
8a _{1g} → 4e _{2u} (F)	CT(M → L)	21 800	
4e _{2g} → 5e _{1g} (A)	d → d	25 150	
4e _{2g} → 5e _{2g} (A)	d → d; CT(M → L) ^d	27 400	31 250
4e _{2g} → 4e _{2u} (A)	CT(M → L)	27 850	
4e _{1g} → 4e _{2u} (A)	L → L	47 750	
4e _{1g} → 5e _{1g} (A)	CT(L → M)	48 300	
4e _{1g} → 5e _{2g} (A)	CT(L → M): L → L ^d	49 200	50 000
6e _{1u} → 4e _{2u} (A)	L → L	51 450	
6e _{1u} → 5e _{1g} (A)	CT(L → M)	52 750	
6e _{1u} → 5e _{2g} (A)	CT(L → M); L → L ^d	53 300	

^a The symbols in parentheses denote orbitally allowed (A) and forbidden (F) transitions. ^b CT = charge transfer; M = metal; L = ligand. ^c Reference 3. ^d Owing to the large mixing of 5e_{2g} MO, this transition cannot be unambiguously assigned to a definite type.

by calculating electronic excitation energies and this will be examined in the next section.

Electronic Excitation Energies of Cr(C₆H₆)₂. Table VIII presents a comparison between calculated electronic excitation energies and corresponding peak positions in the optical and UV absorption spectra²⁵ of Cr(C₆H₆)₂. The MS X α values have been calculated by the transition state procedure,⁴⁸ which means that the major part of orbital relaxation effects accompanying the electronic excitation are taken into account. However, the calculations were done in non-spin-polarized form and the values reported are weighted averages of singlet-singlet and singlet-triplet transition energies. No attempt has been made at determining singlet-triplet splittings since it requires performing additional spin-polarized calculations and previous MS X α calculations³⁶ have shown that singlet-singlet transitions lie at slightly larger energies (0.1–0.2 eV) than these average values. We can thus consider the calculated values of Table VIII as lower limits to MS X α singlet-singlet excitation energies which are likely to be larger by 1000–2000 cm⁻¹. The experimental peak positions of Table VIII are those deduced by Warren³ from an analysis of the optical and UV absorption spectra of Cr(C₆H₆)₂ in cyclohexane solution reported by Feltham,²⁵ except for the second band, with maximum at about 24 000 cm⁻¹, which we have deduced from the visible part of the spectrum of Feltham showing a rising absorption in this region.

It is well known^{3,28} that in such complexes with an unfilled d-electron shell of a metal a few absorption bands of low intensity appear in the visible or near-UV region of the spectrum. These bands may be ascribed to ligand field (or d-d) transitions, as they involve electronic excitations between "d-like" orbitals. Examination of the spectrum reported by Feltham²⁵ suggests that the low-intensity band in the visible with maximum at 15 600 cm⁻¹ is of that type and this is confirmed by the MS X α calculations. We predict the lowest transition in Cr(C₆H₆)₂ to be due to the d-d orbital excitation 8a_{1g} → 5e_{1g} (¹A_{1g} → ¹E_{1g}) and to occur at 16 050 cm⁻¹, in excellent agreement with this experimental value. Owing to the electronic structure of unoccupied levels of Cr(C₆H₆)₂ (see Table V), which shows that the "d-like" and ligand type orbitals lie very close to one another in energy, it is not unexpected to find the next d-d transitions in the vicinity of metal to ligand charge transfer excitations. Thus, as indicated in Table VIII, the

Table IX. Ground-State Energy Levels^a (Ry) and Charge Distribution for Cr(C₆H₆)₂^{+b}

Orbital	Energy	Charge distribution, ^c %									
		Cr			C			H	Empty sphere	Inter-sphere	Outer sphere
		s	p	d	s	pσ	pπ	s			
3b _{2g}	-0.232						74				26
6e _{2g}	-0.255			1	5	2	8				35
3b _{1u}	-0.297						72				28
9a _{1g}	-0.390				5	4	2		1		50
4e _{2u}	-0.469						73				27
5e _{2g}	-0.485			30		1	41				27
5e _{1g}	-0.548			72	1	3	13				10
8a _{1g}	-0.697			79		2		1	2		16
4e _{2g}	-0.747			56		1	15				28
4e _{1g}	-0.911			15			51				33
6e _{1u}	-0.932		1				50				49
6a _{2u}	-1.031		1				63		1		33
3e _{2g}	-1.034				1	60		17			20
3e _{2u}	-1.036				1	59		17			23
7a _{1g}	-1.104		1			1	56		1		38
3e _{1g}	-1.191			2			57	17	3		18
5e _{1u}	-1.194						58	17	3		19
2b _{2g}	-1.209				29	20		22			29
2b _{1u}	-1.223				28	19		22			31
1b _{1g}	-1.334						95				5
1b _{2u}	-1.338						95				5
5a _{2u}	-1.372				5	49		16	5		23
6a _{1g}	-1.396			1	6	46		15	6		24
2e _{su}	-1.564				45	36		6			13
2e _{2g}	-1.573				45	35		5			14
2e _{1g}	-1.855			1	74	12		2	3		8
4e _{1u}	-1.856				74	11		3	3		9
4a _{2u}	-2.081		1		76	9		1	9		4
5a _{1g}	-2.104			1	75	9			9		5
3e _{1u}	-3.901		96								4
3a _{2u}	-3.908		95						1		4
Cr 3s	-5.946	100									
Cr 1s	-20.289			100							
Cr 2p	-41.638		100								
Cr 2s	-48.804	100									
Cr 1s	-428.982	100									

^a The highest occupied level is 8a_{1g}, which contains one electron. ^b The C, H, and empty sphere charge distributions refer to the charge contained in all the respective spheres of the same type. ^c The analysis of charge distribution inside atomic spheres is made according to angular momentum contributions to the total charge inside these spheres.

second band of the spectrum (having a maximum at 24 000 cm⁻¹) with moderate intensity is assigned to the transitions 8a_{1g} → 5e_{2g} and 8a_{1g} → 4e_{2u}, the first of which being in the same time of d-d and metal to ligand charge transfer type (due to the large mixing of 5e_{2g} MO) and the second being unambiguously a charge transfer transition. These excitations are orbitally forbidden, which supports their identification with a band of moderate intensity. The third band of the spectrum (31 250 cm⁻¹) is a strong one which is clearly allowed by both the Laporte and orbital symmetry criteria. Our prediction is that it has mainly to be attributed to the metal to ligand charge transfer transition 4e_{2g} → 4e_{2u} which satisfies these two conditions, though the Laporte-forbidden transitions 4e_{2g} → 5e_{1g} and 4e_{2g} → 5e_{2g} are in the same energy range and could possibly contribute to the overall band intensity. It is worth mentioning that the agreement between the calculated 4e_{2g} → 4e_{2u} transition energy (27 850 cm⁻¹) and corresponding peak position (31 250 cm⁻¹) is again very good. Finally the UV absorption spectrum of Cr(C₆H₆)₂²⁵ reveals an intense absorption beginning at 50 000 cm⁻¹. Our calculation shows that there are three Laporte and orbitally allowed transitions in this region: 4e_{1g} → 4e_{2u} (ligand to ligand) at 47 750 cm⁻¹, 6e_{1u} → 5e_{1g} (ligand to metal charge transfer) at 52 750 cm⁻¹, and 6e_{1u} → 5e_{2g} (ligand to metal charge transfer and ligand to ligand) at 53 300 cm⁻¹. The presence of these three allowed transitions near 50 000 cm⁻¹ explains undoubtedly the experimental evidence of intense rising absorption. As a conclusion, the

agreement with experiment may be considered remarkable for the four bands of the spectrum, the calculated excitation energies being quite close to experimental peak positions, and the Laporte and dipole selection rules explaining the intensities of absorption bands as well.

Ground State Electronic Structure of Cr(C₆H₆)₂⁺. The ground electronic state of Cr(C₆H₆)₂⁺ is predicted to be ²A_{1g}(4e_{2g})⁴(8a_{1g})¹ and the electronic energy levels together with an analysis of their charge distribution in the various regions of the cluster are represented in Table IX. On the other hand, an easy comparison of the electronic structures of Cr(C₆H₆)₂ and Cr(C₆H₆)₂⁺ may be found in Figure 1, which displays the highest occupied and lowest unoccupied MOs of both compounds on the same energy scale. As expected, the orbital levels of the cation are found at significantly lower energies than those of the neutral compound, the stabilization being of the order of 5–6 eV for each level. However, there are no important changes in ordering and relative spacings of the MO levels in the two calculations: the only inversion of MO levels is found for the virtual orbitals 4e_{2u} and 5e_{2g} which are very close to one another anyway. For the cation, the sequence of predominantly metal 3d orbitals is again 4e_{2g} (3dδ) < 8a_{1g}(3dσ) < 5e_{1g}(3dπ), where 4e_{2g} is fully occupied, 8a_{1g} contains the unpaired electron, and 5e_{1g} is unoccupied. This result is in agreement with both magnetic moment³ and ESR²⁶ measurements, which show that the unpaired electron occupies an a_{1g} orbital of essentially 3d_{z²} character. It is also in quali-

tative agreement with an extended Hückel calculation performed by Prins and Reinders,²⁶ with this exception that their results predict the unoccupied ligand π orbital $4e_{2u}$ to lie between the $8a_{1g}$ and $5e_{1g}$ MOs. Concerning the electronic structure of "d-like" orbitals, it is clear from Figure 1 that the first d-d excitation will occur at much lower energy in the cation than in neutral species through the $4e_{2g} \rightarrow 8a_{1g}$ transition. This important conclusion is in complete agreement with the electron absorption spectra of both clusters,^{25,27,28} and this will be discussed in detail in the next section.

Examination of Table IX shows that additional unoccupied levels are found above the $9a_{1g}$ MO: $3b_{1u}$ and $3b_{2g}$, which constitute a pair of in-phase and out-of-phase combinations of π^* orbitals of C_6H_6 , and $6e_{2g}$, a diffuse orbital most probably of carbon 3p Rydberg type. When comparing the charge distributions of corresponding MOs of $Cr(C_6H_6)_2$ and $Cr(C_6H_6)_2^+$ (i.e., the results of Tables V and IX), it is seen that they are similar, even for "d-like" MOs. However, one may notice that the metal 3d participation in the bonding $4e_{2g}$ and $4e_{1g}$ MOs is somewhat larger in the cation, which indicates that (1) the amount of back-bonding through the $4e_{2g}$ MO decreases during ionization and (2) at the same time part of the π bonding interactions in the complex is transferred to the $4e_{1g}$ MO. This is not surprising since during ionization the energy gap between unoccupied ligand and "d-like" MOs tends to increase whereas the energy separation between occupied ligand and "d-like" MOs tends to decrease, as can be seen from Figure 1. This means that there is a fair amount of charge relaxation accompanying the ionization and this is emphasized by a calculation of chromium configuration in $Cr(C_6H_6)_2^+$ using the same procedure as described above for distributing the interatomic charge. The result is $3d^{4.96}$ ($d_{z^2}^{0.94}$, $d_{x^2-y^2}^{1.56}$, $d_{xz}^{0.45}$), the charge on chromium being +1.04, resulting from (1) a transfer of 0.90e from $2p\pi$ orbitals of benzene rings to metal orbitals d_{xz} and d_{yz} and (2) a back-bonding transfer of 0.94e from metal d_{z^2} , $d_{x^2-y^2}$, d_{xy} to ligand $2p\pi$ orbitals. This is to be compared with the chromium configuration $3d^{5.14}$ we have previously obtained for $Cr(C_6H_6)_2$, showing that there is a charge transfer relaxation toward the d shell of the metal during ionization. This conclusion is strengthened by the results of Table VI displaying total electronic charges in the various regions of both neutral and ionized clusters. It is seen there that the electronic charge in the chromium sphere is very much the same in both clusters while there is a drastic decrease of the charge in the interatomic region occurring during ionization. As could be inferred from previous calculations^{11,12} performed on ferrocene, these results show that there is a considerable electronic relaxation accompanying ionization from a predominantly metal 3d orbital in these organometallic compounds. It is thus fully justified to perform separate SCF calculations on the different ionic states of these complexes since their electronic structure can be significantly different from that of the ground state.

Electronic Excitation Energies of $Cr(C_6H_6)_2^+$. The calculation of electronic excitation energies of $Cr(C_6H_6)_2^+$ may be considered as a good test of the validity of the MS X α model in predicting the electronic structure of such "sandwich-type" organometallics. Indeed several absorption bands in the optical and UV spectra of this compound in aqueous solution have been so far reported^{25,27,28} and the positions of these absorption peaks have been generally determined accurately. The comparison between MS X α predictions and experiment is presented in Table X. As for the neutral compound, no attempt has been made to estimate multiplet splittings in the MS X α calculations and our predictions are thus weighted averages of doublet-doublet and doublet-quadruplet transition energies.

The origin of the low-energy band of the near-infrared spectrum, with a maximum at 8500 cm^{-1} and a very weak

Table X. Comparison between Electronic Excitation Energies (cm^{-1}) Calculated for $Cr(C_6H_6)_2^+$ and Experimental Values of Peak Positions

Transition	Type of transition ^a	Calcd value	Exptl peak position ^b
$4e_{2g} \rightarrow 8a_{1g}$ ^c	d \rightarrow d	5800	8500
$8a_{1g} \rightarrow 5e_{1g}$	d \rightarrow d	16 450	17 300 ^d
$4e_{2g} \rightarrow 5e_{1g}$	d \rightarrow d	22 000	
$8a_{1g} \rightarrow 5e_{2g}$	CT(M \rightarrow L); d-d ^e	24 750	25 300 ^d
$4e_{1g} \rightarrow 8a_{1g}$	CT(L \rightarrow M)	25 950	
$6e_{1u} \rightarrow 8a_{1g}$	CT(L \rightarrow M)	29 300	29 400
$4e_{2g} \rightarrow 4e_{2u}$	CT(M \rightarrow L)	32 650	37 000
$6a_{2u} \rightarrow 8a_{1g}$	CT(M \rightarrow L)	40 150	42 600
$6e_{1u} \rightarrow 5e_{1g}$	CT(M \rightarrow L)	45 350	
$4e_{1g} \rightarrow 4e_{2u}$	L \rightarrow L	48 600	
$6e_{1u} \rightarrow 5e_{2g}$	L \rightarrow L; CT(L \rightarrow M) ^e	49 600	50 000
$4e_{2g} \rightarrow 3b_{1u}$	CT(M \rightarrow L)	51 500	

^a CT = charge transfer; M = metal; L = ligand. ^b Reference 25 (unless otherwise stated). ^c Orbital forbidden transition. ^d Reference 28. ^e Owing to the large mixing of $5e_{2g}$ MO, this transition cannot be unambiguously assigned to a definite type.

intensity, is controversial. The interpretation of Feltham²⁵ is that of a symmetry-forbidden excitation of a d electron to a ligand π level, whereas Scott and Becker²⁹ assign this peak to a d-d ($3d\delta \rightarrow 3d\sigma$) transition. Our calculation fully supports the latter interpretation as it shows that there is only one transition in this low-energy region, namely, $4e_{2g} \rightarrow 8a_{1g}$ (${}^2A_{1g} \rightarrow {}^2E_{2g}$), the type of which is d-d ($3d\delta \rightarrow 3d\sigma$). The calculated value of this excitation is 5800 cm^{-1} , i.e., 2700 cm^{-1} less than experiment, but as there is no other excitation at low energy and the first metal to ligand charge transfer excitation occurs at $24\,750\text{ cm}^{-1}$, there is little doubt that the interpretation of Feltham can be discarded on the basis of the present calculations. Furthermore, our calculations suggest that the intensity associated with this transition is very weak since it is both orbitally and Laporte forbidden, and this is in agreement with experiment. According to Yamada et al.,²⁸ two absorption bands are found at higher energies, in the region separating this low-energy band from the intense UV absorption peaks. The first one, with a maximum at $17\,300\text{ cm}^{-1}$, is extremely weak and our calculations suggest that it is associated with the d-d transition $8a_{1g} \rightarrow 5e_{1g}$ (calculated at $16\,450\text{ cm}^{-1}$); the second one, having its maximum at $25\,300\text{ cm}^{-1}$, is in fact a shoulder of moderate intensity on the first intense UV absorption peak and we predict it to originate from three transitions: the d-d excitation $4e_{2g} \rightarrow 5e_{1g}$ (calculated at $22\,000\text{ cm}^{-1}$), the metal to ligand charge transfer and also partly d-d transition $8a_{1g} \rightarrow 5e_{2g}$ (calculated at $24\,750\text{ cm}^{-1}$), and the ligand to metal charge transfer $4e_{1g} \rightarrow 8a_{1g}$ (calculated at $25\,950\text{ cm}^{-1}$). For these two bands, the agreement between calculated excitation energies and experimental peak positions is excellent, the Laporte forbidden nature of the transitions accounting for their weak intensities as well, the second band being stronger owing to the existence of three separate electronic origins.

The UV part of the absorption spectrum^{25,28} of $Cr(C_6H_6)_2^+$ shows three well-defined and intense bands with maxima at $29\,400$, $37\,000$, and $42\,600\text{ cm}^{-1}$ with a rising absorption near $50\,000\text{ cm}^{-1}$. There is no doubt that the origin of these features has to be found in orbitally and Laporte allowed transitions of charge transfer nature. Therefore we have reported in Table X all the calculated transitions of this kind occurring in this energy range, discarding thus numerous additional forbidden transitions. We interpret thus the band at $29\,400\text{ cm}^{-1}$ as being associated with the ligand to metal charge transfer transition $6e_{1u} \rightarrow 8a_{1g}$ (calculated at $29\,300\text{ cm}^{-1}$); the absorption band at $37\,000\text{ cm}^{-1}$ is predicted as originating from the metal to ligand charge transfer transition $4e_{2g} \rightarrow 4e_{2u}$ (calculated at

32 650 cm^{-1}) and the band at 42 600 cm^{-1} is most likely associated with the metal to ligand charge transfer transitions $6a_{2u} \rightarrow 8a_{1g}$ and $6e_{1u} \rightarrow 5e_{1g}$ (predicted to lie at 40 150 and 45 350 cm^{-1} , respectively). Finally, the rising absorption in the spectrum near 50 000 cm^{-1} may be attributed to three different electronic excitations: the ligand to ligand transition $4e_{2g} \rightarrow 4e_{2u}$ (calculated at 48 600 cm^{-1}), the ligand to ligand and also partly ligand to metal charge transfer transition $6e_{1u} \rightarrow 5e_{2g}$ (calculated at 49 600 cm^{-1}), and the metal to ligand charge transfer transition $4e_{2g} \rightarrow 3b_{1u}$ (calculated at 51 500 cm^{-1}). Again, for the UV part of the spectrum, the agreement between our calculated transitions and the positions of absorption band is very good and on the whole the electronic structures of $\text{Cr}(\text{C}_6\text{H}_6)_2$ and $\text{Cr}(\text{C}_6\text{H}_6)_2^+$ as calculated in the MS $X\alpha$ model lead to very satisfactory interpretations of the absorption spectra. This adds credence to the validity of the model for predicting the electronic structure and related properties of "sandwich-type" organometallics.

As a conclusion, let us point out that (1) the same set of MS $X\alpha$ parameters is capable of predicting accurate one-electron properties of both $\text{Cr}(\text{C}_6\text{H}_6)_2$ and its cation and (2) the optimum set of parameters for benzene ligands in $\text{Cr}(\text{C}_6\text{H}_6)_2$ is the same as that of the free benzene molecule, which suggests that the problem of choosing adequate MS $X\alpha$ calculation parameters for large compounds may be solved by performing test calculations on molecular fragments.

Acknowledgment. The Computer Center of the University of Geneva is gratefully acknowledged for a grant of computer time.

Reference and Notes

- (1) (a) Université de Genève; (b) Ecole Supérieure de Chimie de Mulhouse.
- (2) M. E. Watts, *Organomet. Chem.*, **3**, 342 (1975), and references cited therein.
- (3) K. D. Warren, *Struct. Bonding (Berlin)*, **27**, 45 (1976), and references cited therein.
- (4) E. M. Shustorovich and M. E. Dyatkina, *Zh. Strukt. Khim.*, **1**, 98 (1960).
- (5) J. P. Dahl and C. J. Ballhausen, *K. Dan. Vidensk. Selsk., Mat.-Fys. Medd.*, **33**, 5 (1961).
- (6) R. D. Fischer, *Theor. Chim. Acta*, **1**, 418 (1963).
- (7) J. H. Schachtschneider, R. Prins, and P. Ros, *Inorg. Chim. Acta*, **1**, 462 (1967).
- (8) A. T. Armstrong, D. G. Carroll, and S. P. McGlynn, *J. Chem. Phys.*, **47**, 1104 (1967).
- (9) I. H. Hillier and R. M. Canadine, *Discuss. Faraday Soc.*, **47**, 27 (1969).
- (10) A. Botrel, P. Dibout, and R. Lissillour, *Theor. Chim. Acta*, **37**, 37 (1975).
- (11) P. S. Bagus, U. I. Wahlgren, and J. Almlöf, *J. Chem. Phys.*, **64**, 2324 (1976).

- (12) M. M. Coutière, J. Demuyck, and A. Veillard, *Theor. Chim. Acta*, **27**, 281 (1972).
- (13) E. J. Baerends and P. Ros, *Chem. Phys. Lett.*, **23**, 391 (1973).
- (14) N. Rösch and K. H. Johnson, *Chem. Phys. Lett.*, **24**, 179 (1974).
- (15) J. W. Rabalais, L. O. Werme, T. Bergmark, L. Karlsson, M. Hussain, and K. Siegbahn, *J. Chem. Phys.*, **57**, 1185 (1972).
- (16) J. C. Slater, "Quantum Theory of Molecules and Solids", McGraw-Hill, New York, N.Y., 1974.
- (17) K. H. Johnson, *Adv. Quantum Chem.*, **7**, 143 (1973).
- (18) E. Keulen and F. Jellinek, *J. Organomet. Chem.*, **5**, 490 (1966).
- (19) A. Haaland, *Acta Chem. Scand.*, **19**, 41 (1965).
- (20) L. H. Ngai, F. E. Stafford, and L. Schäfer, *J. Am. Chem. Soc.*, **91**, 48 (1969).
- (21) S. Evans, J. C. Green, and S. E. Jackson, *J. Chem. Soc., Faraday Trans. 2*, 249 (1972).
- (22) H. Binder and C. Elschenbroich, *Angew. Chem., Int. Ed. Engl.*, **12**, 659 (1973).
- (23) S. Pignataro, A. Foffani, and G. Distefano, *Chem. Phys. Lett.*, **20**, 350 (1973).
- (24) M. F. Guest, I. H. Hillier, B. R. Higginson, and D. R. Lloyd, *Mol. Phys.*, **29**, 113 (1975).
- (25) R. D. Feltham, *J. Inorg. Nucl. Chem.*, **16**, 197 (1961).
- (26) R. Prins and F. J. Reinders, *Chem. Phys. Lett.*, **3**, 45 (1969).
- (27) S. Yamada, H. Nakamura, and R. Tsuchida, *Bull. Chem. Soc. Jpn.*, **30**, 647 (1957).
- (28) S. Yamada, H. Yamazaki, H. Nishikawa, and R. Tsuchida, *Bull. Chem. Soc. Jpn.*, **33**, 481 (1960).
- (29) D. R. Scott and R. S. Becker, *J. Phys. Chem.*, **69**, 3207 (1965).
- (30) E. M. Shustorovich and M. E. Dyatkina, *Dokl. Akad. Nauk SSSR*, **128**, 1234 (1959).
- (31) S. E. Anderson and R. S. Drago, *Inorg. Chem.*, **11**, 1564 (1972).
- (32) J. Y. Saillard, D. Grandjean, F. Choplin, and G. Kaufmann, *J. Mol. Struct.*, **23**, 363, (1974).
- (33) N. J. Fitzpatrick, J. M. Savariault, and J. F. R. Labarre, *J. Organomet. Chem.*, **127**, 325 (1977).
- (34) K. H. Johnson and R. P. Messmer, *Int. J. Quantum Chem., Symp.*, **10**, 147 (1976), and references cited therein.
- (35) V. A. Gubanov, J. Weber, and J. W. D. Connolly, *J. Chem. Phys.*, **63**, 1455 (1975).
- (36) J. Weber, *Chem. Phys. Lett.*, **45**, 261 (1977).
- (37) J. Weber, H. Berthou, and C. K. Jørgensen, *Chem. Phys. Lett.*, **45**, 1 (1977).
- (38) J. Weber, H. Berthou, and C. K. Jørgensen, *Chem. Phys.*, **26**, 69 (1977).
- (39) M. Boring and J. W. Moskowitz, *Chem. Phys. Lett.*, **38**, 185 (1976).
- (40) J. B. Danese and J. W. D. Connolly, *J. Chem. Phys.*, **61**, 3063 (1974).
- (41) J. Weber, *Chem. Phys. Lett.*, **40**, 275 (1976).
- (42) J. Weber and M. Geoffroy, *Theor. Chim. Acta*, **43**, 299 (1977).
- (43) K. Schwarz, *Phys. Rev. Sect. B*, **5**, 2466 (1972).
- (44) K. Schwarz, *Theor. Chim. Acta*, **34**, 225 (1974).
- (45) N. Rösch, W. G. Klempere, and K. H. Johnson, *Chem. Phys. Lett.*, **23**, 149 (1973).
- (46) W. C. Ermler and C. W. Kern, *J. Chem. Phys.*, **58**, 3458 (1973).
- (47) In the C_6H_6 calculation it has been found that the results remain practically unchanged when enlarging the expansions up to $l = 3$ in extramolecular region, up to $l = 2$ in carbon and empty spheres, and up to $l = 1$ in hydrogen sphere.
- (48) J. C. Slater, *Adv. Quantum Chem.*, **6**, 1 (1972).
- (49) M. B. Robin, "Higher Excited States of Polyatomic Molecules", Academic Press, New York, N.Y., 1975, p 210.
- (50) E. E. Koch and A. Otto, *Chem. Phys. Lett.*, **12**, 476 (1972).
- (51) According to the pseudoaxial ligand field theory,³ the d-orbital set in D_{6h} symmetry is split into three irreducible representations: a_{1g} ($\sigma: d_{z^2}$), e_{1g} ($\pi: d_{xz}, d_{yz}$), e_{2g} ($\delta: d_{x^2-y^2}, d_{xy}$), where z is the sixfold rotational axis.
- (52) C. K. Jørgensen and H. Berthou, *Chem. Phys. Lett.*, **31**, 416 (1975).